AIAA JOURNAL
Vol. 46, No. 3, March 2008

Circular Inhomogeneity with Viscoelastic Interface Under Antiplane Shear

X. Wang* and E. Pan†
University of Akron,
Akron, Ohio 44325-3905
and
A. K. Roy‡
U.S. Air Force Research Laboratory,
Wright–Patterson Air Force Base, Ohio 45433-7750

DOI: 10.2514/1.33983

This investigation addresses in detail a circular inhomogeneity with a viscoelastic interface subjected to remote uniform antiplane shear stresses. Both the inhomogeneity and the surrounding matrix are assumed to be elastic and quasi static, and the interface is viscoelastic, modeled by a linear spring and dashpot. Exact closed-form solutions for both the Kelvin- and Maxwell-type viscoelastic interfaces are obtained by means of the complex variable method. It is observed that when the matrix is subjected to remote uniform shear stresses, the stress field inside the inhomogeneity, although time-dependent, is still uniform. The derived solutions are then used to predict the time-dependent effective shear modulus of the composite based on the Mori–Tanaka mean-field approximation.

I. Introduction

COMPOSITES under harsh environments could be damaged during their service, and the need to repair these structures is critical. Although composites can be repaired with adhesively bonded joints, material behaviors of the joint and the bonded composite (in particular, their time-dependent behavior) are challenging [1]. Recently, He [2] and He and Lim [3] studied the time-dependent mechanical responses of a particle- and fiber-reinforced composite with a viscous interface in which the interface model is based on the assumption that the two materials slide at a relative velocity that is proportional to the interface shear stress [4]. It is found that significant stress relaxation occurs, and the effective elastic moduli of the composites change remarkably with time. When time approaches infinity, the viscous interface will become a complete sliding one and would lose the ability of transferring the shear stress totally. As a result, the final overall modulus after complete sliding is independent of the modulus of the fibers [2,3]. In fact, viscoelastic interface, which is modeled by a linear spring and dashpot, is more suitable to characterize the creep and relaxation behavior of interlaminar bonding behavior under high-temperature circumstances [5]. As pointed out by Fan and Wang [6], there exist plenty of cases in which the interface should be considered as viscoelastic. For example, epoxy has a melting temperature in the range of about 340–380 K and when used as an adhesive to join a pair of metals with a high melting temperature (e.g., aluminum with a melting temperature of about 1000 K), it may form an imperfect and viscoelastic interface at room temperature of about 300 K. Most recently, the topic of a composite with a *viscoelastic interface* has attracted a considerable amount of attention [7–10].

In this work, we study the more practical and more complicated case in which a circular inhomogeneity is connected to the matrix by a viscoelastic interface modeled by a linear spring and dashpot [6]. Although both the Kelvin- and Maxwell-type interfaces are considered here, the gradient interface effect will be addressed in a separate paper. We first study an isolated circular inhomogeneity with viscoelastic interface by using the complex variable method and analytical continuation. The uniform far-field-induced stresses and displacements are obtained for the two different viscoelastic interfaces. Then the time-dependent shear modulus of the composite with finite fiber concentration is derived by using the Mori–Tanaka mean-field method [3,11,12]. It is verified that our results can be reduced to those for viscous interface obtained by He and Lim [3] and to those for a linear elastic spring-type interface [13]. Numerical results are presented to illustrate the physics of the obtained solutions.

II. Formulation

As shown in Fig. 1, an isolated circular inhomogeneity of radius R is embedded in an infinite matrix. The center of the circular inhomogeneity is at the origin of the Cartesian coordinate system. Both the inhomogeneity and matrix are assumed to be homogeneous, linearly elastic, and isotropic, with shear moduli μ_1 and μ_2, respectively. The matrix is subjected to remote uniform antiplane shear stresses σ_{zx}^{∞} and σ_{zy}^{∞}, and the inertia force in both the inhomogeneity and matrix is neglected so that the analysis is restricted to a quasi-static process, with the antiplane displacement governed by the two-dimensional Laplace equation. As such, the out-of-plane displacement w (i.e., u_z), the stress components σ_{zx} and σ_{zy} in the Cartesian coordinate system, and the stress components σ_{zr} and $\sigma_{z\theta}$ in the polar coordinate system can be expressed in terms of a single analytic function $f(z,t)$ as [14]

$$w = \mathrm{Im}\{f(z,t)\} \tag{1}$$

$$\sigma_{zy} + \mathrm{i}\sigma_{zx} = \mu f'(z,t) \tag{2}$$

$$\sigma_{z\theta} + \mathrm{i}\sigma_{zr} = \mu e^{\mathrm{i}\theta} f'(z,t) \tag{3}$$

Received 10 August 2007; accepted for publication 5 November 2007. Copyright © 2007 by the American Institute of Aeronautics and Astronautics, Inc. All rights reserved. Copies of this paper may be made for personal or internal use, on condition that the copier pay the $10.00 per-copy fee to the Copyright Clearance Center, Inc., 222 Rosewood Drive, Danvers, MA 01923; include the code 0001-1452/08 $10.00 in correspondence with the CCC.

*Visiting Professor, Department of Civil Engineering; xuwang@uakron.edu (Corresponding Author).

†Associate Professor, Department of Civil Engineering; pan2@uakron.edu.

‡Research Leader, Structural Materials Branch, Materials and Manufacturing Directorate, Building 654, 2941 Hobson Way; Ajit.roy@wpafb.af.mil.

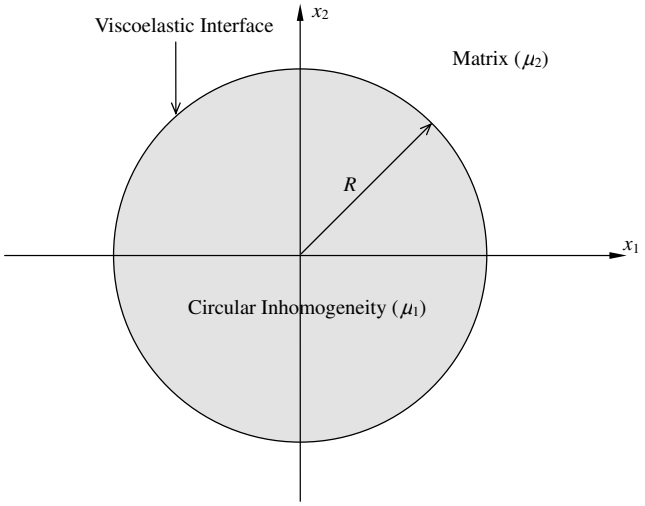

Fig. 1 A circular inhomogeneity within an infinite matrix connected by a viscoelastic interface.

where $z = x + \mathrm{i}y = re^{i\theta}$ is the complex variable, and $f'(z,t) = [\partial f(z,t)]/\partial z$. Because of the effect of the viscoelastic interface, $f(z,t)$ is not only a function of the complex variable z, but also a function of the real-time variable t. In the following the superscripts (1) and (2) will be used to denote stresses and displacement associated with the circular inhomogeneity and the matrix, respectively. In addition, the analytic functions defined in the inhomogeneity and the matrix are denoted by $f_1(z,t)$ ($|z| \le R$) and $f_2(z,t)$ ($|z| \ge R$), respectively.

In this paper, we address both the Kelvin- and Maxwell-type viscoelastic interfaces. The boundary conditions for the Kelvin model, in which a linear spring and a linear dashpot are parallel-connected, are given by [6]

$$\begin{aligned} \sigma_{zr}^{(1)} &= \sigma_{zr}^{(2)} \\ \sigma_{zr}^{(1)} &= k[w^{(2)} - w^{(1)}] + \eta\frac{\partial}{\partial t}[w^{(2)} - w^{(1)}], \quad \text{on } r = R \end{aligned} \tag{4}$$

where k is the spring constant of the interface and η is the viscosity coefficient.

The boundary conditions for the Maxwell model, in which a linear spring and a linear dashpot are connected in series, are given by [6]

$$\sigma_{zr}^{(1)} = \sigma_{zr}^{(2)}, \qquad \frac{\partial}{\partial t}[w^{(2)} - w^{(1)}] = \frac{\sigma_{zr}^{(1)}}{\eta} + \frac{1}{k}\frac{\partial \sigma_{zr}^{(1)}}{\partial t}, \quad \text{on } r = R \tag{5}$$

In the next two sections, we will derive the analytic solutions for the two kinds of viscoelastic interfaces.

III. Solution for a Kelvin-Type Viscoelastic Interface

Equation (4) for the boundary conditions of a Maxwell-type viscoelastic interface can be expressed in terms of two analytic functions $f_1(z,t)$ and $f_2(z,t)$ as

$$\mu_1 f_1^+(z,t) + \mu_1 \bar{f}_1^-\left(\frac{R^2}{z},t\right) = \mu_2 f_2^-(z,t) + \mu_2 \bar{f}_2^+\left(\frac{R^2}{z},t\right) \tag{6a}$$

$$\begin{aligned} &k\left[f_2^-(z,t) - \bar{f}_2^+\left(\frac{R^2}{z},t\right) - f_1^+(z,t) + \bar{f}_1^-\left(\frac{R^2}{z},t\right)\right] \\ &\quad + \eta\frac{\partial}{\partial t}\left[f_2^-(z,t) - \bar{f}_2^+\left(\frac{R^2}{z},t\right) - f_1^+(z,t) + \bar{f}_1^-\left(\frac{R^2}{z},t\right)\right] \\ &\quad = \frac{\mu_1}{R}\left[z f_1'^+(z,t) - \frac{R^2}{z}\bar{f}_1'^-\left(\frac{R^2}{z},t\right)\right] \\ &\qquad |z| = R \end{aligned} \tag{6b}$$

It then follows from Eq. (6a) that

$$\begin{aligned} f_2(z,t) &= \frac{\mu_1}{\mu_2}\bar{f}_1\left(\frac{R^2}{z},t\right) + \frac{\sigma_{zy}^{\infty} + \mathrm{i}\sigma_{zx}^{\infty}}{\mu_2}z - \frac{R^2\left(\sigma_{zy}^{\infty} - \mathrm{i}\sigma_{zx}^{\infty}\right)}{\mu_2}\frac{1}{z} \\ \bar{f}_2\left(\frac{R^2}{z},t\right) &= \frac{\mu_1}{\mu_2}f_1(z,t) - \frac{\sigma_{zy}^{\infty} + \mathrm{i}\sigma_{zx}^{\infty}}{\mu_2}z + \frac{R^2\left(\sigma_{zy}^{\infty} - \mathrm{i}\sigma_{zx}^{\infty}\right)}{\mu_2}\frac{1}{z} \end{aligned} \tag{7}$$

Substituting Eq. (7) into Eq. (6b) and eliminating $f_2^-(z,t)$ and $\bar{f}_2^+[(R^2/z),t]$ results in

$$\begin{aligned} &k\frac{\mu_1+\mu_2}{\mu_2}f_1^+(z,t) + \frac{\mu_1}{R}z f_1'^+(z,t) + \eta\frac{\mu_1+\mu_2}{\mu_2}\frac{\partial}{\partial t}f_1^+(z,t) \\ &\quad - k\frac{2\left(\sigma_{zy}^{\infty} + \mathrm{i}\sigma_{zx}^{\infty}\right)}{\mu_2}z = k\frac{\mu_1+\mu_2}{\mu_2}\bar{f}_1^-\left(\frac{R^2}{z},t\right) \\ &\quad + \frac{\mu_1}{R}\frac{R^2}{z}\bar{f}_1'^-\left(\frac{R^2}{z},t\right) + \eta\frac{\mu_1+\mu_2}{\mu_2}\frac{\partial}{\partial t}\bar{f}_1^-\left(\frac{R^2}{z},t\right) \\ &\quad - k\frac{2\left(\sigma_{zy}^{\infty} - \mathrm{i}\sigma_{zx}^{\infty}\right)}{\mu_2}\frac{R^2}{z}, \qquad |z| = R \end{aligned} \tag{8}$$

It is apparent that the left-hand side of Eq. (8) is analytic within the circle $r = R$, whereas the right-hand side is analytic outside the circle, including the point at infinity. Consequently, the continuity condition in Eq. (8) implies that the left- and right-hand sides of Eq. (8) are identically zero within and outside the circle $r = R$. It then follows that

$$\begin{aligned} &\chi f_1(z,t) + z\frac{\partial f_1(z,t)}{\partial z} + \gamma\frac{\partial f_1(z,t)}{\partial t} \\ &\quad = \frac{2\chi\left(\sigma_{zy}^{\infty} + \mathrm{i}\sigma_{zx}^{\infty}\right)}{\mu_1+\mu_2}z, \qquad |z| \le R \end{aligned} \tag{9}$$

where χ and γ are, respectively, the interface rigidity and the characteristic time, given by

$$\chi = kR\frac{\mu_1+\mu_2}{\mu_1\mu_2}, \qquad \gamma = \eta R\frac{\mu_1+\mu_2}{\mu_1\mu_2} \tag{10}$$

At time $t = 0$, the displacement across the interface has no time to experience any jump, due to the dashpot [3,6]. Therefore, at the initial time $t = 0$, the interface is a perfect one. As a result, we have

$$f_1(z,0) = \frac{2\left(\sigma_{zy}^{\infty} + \mathrm{i}\sigma_{zx}^{\infty}\right)}{\mu_1+\mu_2}z \tag{11}$$

When $t \to \infty$, the interface should be at a steady state and there is no time effect. Then it follows from Eq. (9) that

$$\chi f_1(z,\infty) + z\frac{\partial f_1(z,\infty)}{\partial z} = \frac{2\chi\left(\sigma_{zy}^{\infty} + \mathrm{i}\sigma_{zx}^{\infty}\right)}{\mu_1+\mu_2}z \tag{12}$$

for which the solution is expediently given by

$$f_1(z,\infty) = \frac{2\chi\left(\sigma_{zy}^{\infty} + \mathrm{i}\sigma_{zx}^{\infty}\right)}{(\chi+1)(\mu_1+\mu_2)}z \tag{13}$$

In view of Eqs. (11) and (13), the solution to Eq. (9) can be given by

$$f_1(z,t) = \frac{2\left(\sigma_{zy}^{\infty}+\mathrm{i}\sigma_{zx}^{\infty}\right)}{(\chi+1)(\mu_1+\mu_2)}\left[\chi+\exp\left(-\frac{\chi+1}{\gamma}t\right)\right]z, \qquad |z|\le R \tag{14}$$

Consequently, the expression of $f_2(z,t)$ is

$$f_2(z,t) = \frac{\left(\sigma_{zy}^{\infty}-\mathrm{i}\sigma_{zx}^{\infty}\right)}{\mu_2}\left[\frac{\chi(\mu_1-\mu_2)-(\mu_1+\mu_2)}{(\chi+1)(\mu_1+\mu_2)} + \frac{2\mu_1}{(\chi+1)(\mu_1+\mu_2)}\exp\left(-\frac{\chi+1}{\gamma}t\right)\right]\frac{R^2}{z} + \frac{\sigma_{zy}^{\infty}+\mathrm{i}\sigma_{zx}^{\infty}}{\mu_2}z, \qquad |z|\ge R \tag{15}$$

Inserting the preceding two expressions for $f_1(z,t)$ and $f_2(z,t)$ into Eq. (1), we can obtain the time-dependent displacement and stress fields in the inhomogeneity and the matrix as

$$w^{(1)} = \frac{2}{(\chi+1)(\mu_1+\mu_2)} \times\left[\chi+\exp\left(-\frac{\chi+1}{\gamma}t\right)\right]r\left(\sigma_{zy}^{\infty}\sin\theta+\sigma_{zx}^{\infty}\cos\theta\right)$$
$$w^{(2)} = \left[1+\frac{\mu_1+\mu_2+\chi(\mu_2-\mu_1)}{(\chi+1)(\mu_1+\mu_2)}\left(\frac{R}{r}\right)^2 - \frac{2\mu_1}{(\chi+1)(\mu_1+\mu_2)}\left(\frac{R}{r}\right)^2\exp\left(-\frac{\chi+1}{\gamma}t\right)\right] \times\frac{r\left(\sigma_{zy}^{\infty}\sin\theta+\sigma_{zx}^{\infty}\cos\theta\right)}{\mu_2} \tag{16}$$

$$\sigma_{zy}^{(1)}+\mathrm{i}\sigma_{zx}^{(1)} = \frac{2\mu_1\left(\sigma_{zy}^{\infty}+\mathrm{i}\sigma_{zx}^{\infty}\right)}{(\chi+1)(\mu_1+\mu_2)}\left[\chi+\exp\left(-\frac{\chi+1}{\gamma}t\right)\right] \tag{17a}$$

$$\sigma_{zy}^{(2)}+\mathrm{i}\sigma_{zx}^{(2)} = \sigma_{zy}^{\infty}+\mathrm{i}\sigma_{zx}^{\infty} + \left(\sigma_{zy}^{\infty}-\mathrm{i}\sigma_{zx}^{\infty}\right)\left[\frac{\mu_1+\mu_2+\chi(\mu_2-\mu_1)}{(\chi+1)(\mu_1+\mu_2)} - \frac{2\mu_1}{(\chi+1)(\mu_1+\mu_2)}\exp\left(-\frac{\chi+1}{\gamma}t\right)\right]\frac{R^2}{z^2} \tag{17b}$$

It is observed from Eq. (17a) that the stress field inside the circular inhomogeneity with the Kelvin-type interface is still uniform, although the uniform stress field is time-dependent. We further remark that our general solution contains various existing results as special cases, as presented next.

1) When $k=0$ for a viscous interface, we have $\chi=0$. Then Eqs. (16) and (17) reduce to

$$w^{(1)} = \frac{2}{\mu_1+\mu_2}\exp\left(-\frac{t}{\gamma}\right)r\left(\sigma_{zy}^{\infty}\sin\theta+\sigma_{zx}^{\infty}\cos\theta\right)$$
$$w^{(2)} = \left[1+\left(\frac{R}{r}\right)^2 - \frac{2\mu_1}{\mu_1+\mu_2}\left(\frac{R}{r}\right)^2\exp\left(-\frac{t}{\gamma}\right)\right]\frac{r\left(\sigma_{zy}^{\infty}\sin\theta+\sigma_{zx}^{\infty}\cos\theta\right)}{\mu_2} \tag{18}$$

$$\sigma_{zy}^{(1)}+\mathrm{i}\sigma_{zx}^{(1)} = \frac{2\mu_1\left(\sigma_{zy}^{\infty}+\mathrm{i}\sigma_{zx}^{\infty}\right)}{\mu_1+\mu_2}\exp\left(-\frac{t}{\gamma}\right)$$
$$\sigma_{zy}^{(2)}+\mathrm{i}\sigma_{zx}^{(2)} = \sigma_{zy}^{\infty}+\mathrm{i}\sigma_{zx}^{\infty}+\left(\sigma_{zy}^{\infty}-\mathrm{i}\sigma_{zx}^{\infty}\right) \times\left[1-\frac{2\mu_1}{\mu_1+\mu_2}\exp\left(-\frac{t}{\gamma}\right)\right]\frac{R^2}{z^2} \tag{19}$$

which are in agreement with those derived by He and Lim [3] if we let $\sigma_{zx}^{\infty}=0$.

2) When $\eta=0$ for a linear-spring model, we have $\gamma=0$. In this case, Eqs. (16) and (17) reduce to

$$w^{(1)} = \frac{2\chi r\left(\sigma_{zy}^{\infty}\sin\theta+\sigma_{zx}^{\infty}\cos\theta\right)}{(\chi+1)(\mu_1+\mu_2)}$$
$$w^{(2)} = \left[1+\frac{\mu_1+\mu_2+\chi(\mu_2-\mu_1)}{(\chi+1)(\mu_1+\mu_2)}\left(\frac{R}{r}\right)^2\right] \times\frac{r\left(\sigma_{zy}^{\infty}\sin\theta+\sigma_{zx}^{\infty}\cos\theta\right)}{\mu_2} \tag{20}$$

$$\sigma_{zy}^{(1)}+\mathrm{i}\sigma_{zx}^{(1)} = \frac{2\mu_1\chi\left(\sigma_{zy}^{\infty}+\mathrm{i}\sigma_{zx}^{\infty}\right)}{(\chi+1)(\mu_1+\mu_2)}$$
$$\sigma_{zy}^{(2)}+\mathrm{i}\sigma_{zx}^{(2)} = \sigma_{zy}^{\infty}+\mathrm{i}\sigma_{zx}^{\infty} + \left(\sigma_{zy}^{\infty}-\mathrm{i}\sigma_{zx}^{\infty}\right)\frac{\mu_1+\mu_2+\chi(\mu_2-\mu_1)}{(\chi+1)(\mu_1+\mu_2)}\frac{R^2}{z^2} \tag{21}$$

which coincide with those derived by Ru and Schiavone [13].

In Fig. 2, to show the basic feature of the obtained solution, we demonstrate the continuous variation of σ_{zx} along the positive real axis at four different moments [$t=0$, $\gamma/(\chi+1)$, $1.6094\gamma/(\chi+1)$, and ∞] for the Kelvin-type interface. The matrix is subjected to σ_{zx}^{∞} and the other fixed parameters are $\chi=1$ and $\mu_1=5\mu_2$. It is observed that at the initial time ($t=0$), the stress level within the fiber is rather high ($\sigma_{zx}^{(1)}=\frac{5}{3}\sigma_{zx}^{\infty}>\sigma_{zx}^{\infty}$). With increasing time, the stress level within the inhomogeneity decreases. When $t=1.6094\gamma/(\chi+1)$, the stress is just equal to σ_{zx}^{∞} everywhere along the real axis. At this moment, the existence of the stiff inhomogeneity does not disturb the uniform stress field in the matrix, due to the viscoelastic interface. When $t\to\infty$, the stress approaches the steady state $\sigma_{zx}^{(1)}=\frac{5}{6}\sigma_{zx}^{\infty}<\sigma_{zx}^{\infty}$: namely, the result for a linear-spring-type interface.

By using the Mori–Tanaka mean-field method [3,11,12] with the intermediate procedures ignored, the time-dependent effective shear modulus of a composite containing randomly aligned fibers of the same radius with a Kelvin-type interface on the x–y plane can be derived to be

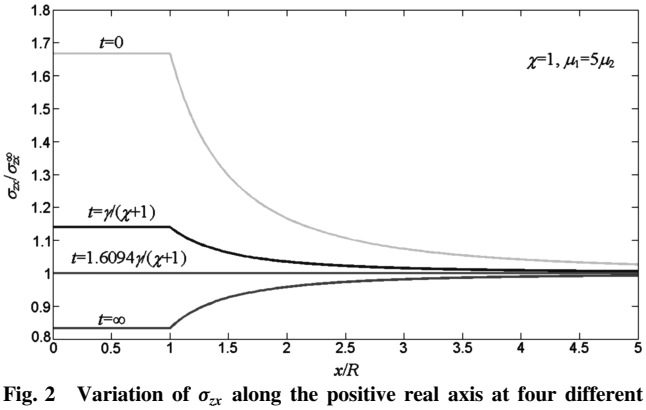

Fig. 2 Variation of σ_{zx} along the positive real axis at four different moments [$t=0$, $\gamma/(\chi+1)$, $1.6094\gamma/(\chi+1)$, and ∞] for the Kelvin-type interface, in which the matrix is subjected to σ_{zx}^{∞} with the fixed parameters $\chi=1$ and $\mu_1=5\mu_2$.

$$\mu^* = \mu_2 \frac{1 - c\left[\dfrac{\mu_1 + \mu_2 + \chi(\mu_2 - \mu_1)}{(\chi+1)(\mu_1+\mu_2)} - \dfrac{2\mu_1}{(\chi+1)(\mu_1+\mu_2)}\exp\left(-\dfrac{\chi+1}{\gamma}t\right)\right]}{1 + c\left[\dfrac{\mu_1 + \mu_2 + \chi(\mu_2 - \mu_1)}{(\chi+1)(\mu_1+\mu_2)} - \dfrac{2\mu_1}{(\chi+1)(\mu_1+\mu_2)}\exp\left(-\dfrac{\chi+1}{\gamma}t\right)\right]} \tag{22}$$

where μ^* is the time-dependent effective shear modulus, and c is the volume fraction of the fiber. It is seen that the effective shear modulus is determined by the shear moduli of the fiber and the matrix, the volume fraction c of the fiber, the interface rigidity χ, and the characteristic time γ. The composite behaves macroscopically like an anelastic body. When $\chi = 0$ for a viscous interface, Eq. (22) reduces to

$$\mu^* = \mu_2 \frac{1 - c\left[1 - \dfrac{2\mu_1}{\mu_1+\mu_2}\exp\left(-\dfrac{t}{\gamma}\right)\right]}{1 + c\left[1 - \dfrac{2\mu_1}{\mu_1+\mu_2}\exp\left(-\dfrac{t}{\gamma}\right)\right]} \tag{23}$$

which is just the result derived by He and Lim [3].

In Fig. 3, we plot the variation of μ^* as a function of time t for the Kelvin-type interface with $\chi = 1$ and $\mu_1 = 10\mu_2$. Comparing Fig. 3 for the Kelvin-type viscoelastic interface with Fig. 5 in He and Lim [3] for a viscous interface ($\chi = 0$), it is found that the loss of the overall shear modulus for a Kelvin-type viscoelastic interface is not as large as that for a viscous interface, due to the fact that the Kelvin-type viscoelastic interface will finally evolve into a linear spring-type interface, whereas a viscous interface will finally evolve into a traction-free surface (or complete sliding interface).

IV. Solution for a Maxwell-Type Viscoelastic Interface

Equation (5) for the boundary conditions on a Maxwell-type viscoelastic interface can be expressed in terms of the two analytic functions $f_1(z,t)$ and $f_2(z,t)$ as

$$\mu_1 f_1^+(z,t) + \mu_1 \bar{f}_1^-\left(\frac{R^2}{z},t\right) = \mu_2 f_2^-(z,t) + \mu_2 \bar{f}_2^+\left(\frac{R^2}{z},t\right) \tag{24a}$$

$$\begin{aligned}&\frac{\partial}{\partial t}\left[f_2^-(z,t) - \bar{f}_2^+\left(\frac{R^2}{z},t\right) - f_1^+(z,t) + \bar{f}_1^-\left(\frac{R^2}{z},t\right)\right]\\ &\quad = \frac{\mu_1}{R\eta}\left[z f_1'^+(z,t) - \frac{R^2}{z}\bar{f}_1'^-\left(\frac{R^2}{z},t\right)\right]\\ &\quad + \frac{\mu_1}{Rk}\frac{\partial}{\partial t}\left[z f_1'^+(z,t) - \frac{R^2}{z}\bar{f}_1'^-\left(\frac{R^2}{z},t\right)\right]\end{aligned} \tag{24b}$$

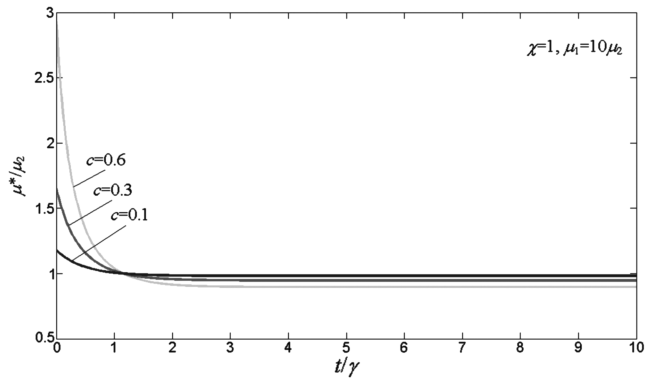

Fig. 3 Variation of μ^* as a function of time t for the Kelvin-type viscoelastic interface with $\chi = 1$ and $\mu_1 = 10\mu_2$.

Similar to the analysis in the previous section, it follows from Eq. (24a) that

$$\begin{aligned}f_2(z,t) &= \frac{\mu_1}{\mu_2}\bar{f}_1\left(\frac{R^2}{z},t\right) + \frac{\sigma_{zy}^\infty + \mathrm{i}\sigma_{zx}^\infty}{\mu_2}z - \frac{R^2\left(\sigma_{zy}^\infty - \mathrm{i}\sigma_{zx}^\infty\right)}{\mu_2}\frac{1}{z}\\ \bar{f}_2\left(\frac{R^2}{z},t\right) &= \frac{\mu_1}{\mu_2}f_1(z,t) - \frac{\sigma_{zy}^\infty + \mathrm{i}\sigma_{zx}^\infty}{\mu_2}z + \frac{R^2\left(\sigma_{zy}^\infty - \mathrm{i}\sigma_{zx}^\infty\right)}{\mu_2}\frac{1}{z}\end{aligned} \tag{25}$$

Substituting Eq. (25) into Eq. (24b) and eliminating $f_2^-(z,t)$ and $\bar{f}_2^+[(R^2/v),t]$ will result in

$$\begin{aligned}&\frac{\mu_1+\mu_2}{\mu_2}\frac{\partial}{\partial t}f_1^+(z,t) + \frac{\mu_1}{R\eta}z f_1'^+(z,t) + \frac{\mu_1}{Rk}z\frac{\partial}{\partial t}f_1'^+(z,t)\\ &\quad = \frac{\mu_1+\mu_2}{\mu_2}\frac{\partial}{\partial t}\bar{f}_1^-\left(\frac{R^2}{z},t\right) + \frac{\mu_1}{R\eta}\frac{R^2}{z}\bar{f}_1'^-\left(\frac{R^2}{z},t\right)\\ &\quad + \frac{\mu_1}{Rk}\frac{R^2}{z}\frac{\partial}{\partial t}\bar{f}_1'^-\left(\frac{R^2}{z},t\right)\end{aligned} \tag{26}$$

It is apparent that the left-hand side of Eq. (26) is analytic within the circle $r = R$, while the right-hand side is analytic outside the circle, including the point at infinity. Consequently the continuity condition in Eq. (26) implies that the left- and right-hand sides of Eq. (26) are identically zero within and outside the circle $r = R$. It then follows that

$$\frac{\partial f_1(z,t)}{\partial t} + \frac{1}{\gamma}z\frac{\partial f_1(z,t)}{\partial z} + \frac{1}{\chi}z\frac{\partial^2 f_1(z,t)}{\partial z\partial t} = 0, \qquad |z| \le R \tag{27}$$

where

$$\chi = kR\frac{\mu_1+\mu_2}{\mu_1\mu_2}, \qquad \gamma = \eta R\frac{\mu_1+\mu_2}{\mu_1\mu_2} \tag{28}$$

At the initial time $t = 0$, the dashpot does not deform immediately, and the spring responds to the loading with no time delay. Thus, the displacement across the interface exhibits an immediate jump as the response of a spring [6]. On the other hand, when $t \to \infty$, the interface becomes a traction-free surface. As a result,

$$f_1(z,0) = \frac{2\chi\left(\sigma_{zy}^\infty + \mathrm{i}\sigma_{zx}^\infty\right)}{(\chi+1)(\mu_1+\mu_2)}z, \qquad f_1(z,\infty) = 0 \tag{29}$$

In view of the preceding, the solution to Eq. (27) can be given by

$$f_1(z,t) = \frac{2\chi\left(\sigma_{zy}^\infty + \mathrm{i}\sigma_{zx}^\infty\right)}{(\chi+1)(\mu_1+\mu_2)}\exp\left(-\frac{\chi t}{\gamma(\chi+1)}\right)z \tag{30}$$

and the expression of $f_2(z,t)$ is

$$f_2(z,t) = \frac{\left(\sigma_{zy}^{\infty} - \mathrm{i}\sigma_{zx}^{\infty}\right)}{\mu_2} \times \left[\frac{2\chi\mu_1}{(\chi+1)(\mu_1+\mu_2)}\exp\left(-\frac{\chi t}{\gamma(\chi+1)}\right) - 1\right]\frac{R^2}{z} + \frac{\sigma_{zy}^{\infty} + \mathrm{i}\sigma_{zx}^{\infty}}{\mu_2} z \tag{31}$$

Now that we have obtained $f_1(z,t)$ and $f_2(z,t)$, then it is easy to write down the time-dependent displacement and stress fields as

$$w^{(1)} = \frac{2\chi}{(\chi+1)(\mu_1+\mu_2)}\exp\left(-\frac{\chi t}{\gamma(\chi+1)}\right) \times \left(\sigma_{zy}^{\infty} + \mathrm{i}\sigma_{zx}^{\infty}\right) r\left(\sigma_{zy}^{\infty}\sin\theta + \sigma_{zx}^{\infty}\cos\theta\right)$$

$$w^{(2)} = \left[1 + \left(\frac{R}{r}\right)^2 - \frac{2\chi\mu_1}{(\chi+1)(\mu_1+\mu_2)}\left(\frac{R}{r}\right)^2 \exp\left(-\frac{\chi t}{\gamma(\chi+1)}\right)\right] \times \frac{r(\sigma_{zy}^{\infty}\sin\theta + \sigma_{zx}^{\infty}\cos\theta)}{\mu_2} \tag{32}$$

$$\sigma_{zy}^{(1)} + \mathrm{i}\sigma_{zx}^{(1)} = \frac{2\chi\mu_1\left(\sigma_{zy}^{\infty} + \mathrm{i}\sigma_{zx}^{\infty}\right)}{(\chi+1)(\mu_1+\mu_2)}\exp\left(-\frac{\chi t}{\gamma(\chi+1)}\right) \tag{33a}$$

$$\sigma_{zy}^{(2)} + \mathrm{i}\sigma_{zx}^{(2)} = \sigma_{zy}^{\infty} + \mathrm{i}\sigma_{zx}^{\infty} + \left(\sigma_{zy}^{\infty} - \mathrm{i}\sigma_{zx}^{\infty}\right)\left[1 - \frac{2\chi\mu_1}{(\chi+1)(\mu_1+\mu_2)}\exp\left(-\frac{\chi t}{\gamma(\chi+1)}\right)\right]\frac{R^2}{z^2} \tag{33b}$$

Similarly, it is observed from Eq. (33a) that the stress field inside the circular inhomogeneity with the Maxwell-type interface is still uniform, although the uniform stress field is time-dependent. In Fig. 4, we demonstrate the continuous variation of σ_{zx} along the positive real axis at three different moments $t = 0, [\gamma(\chi+1)]/\chi$, and ∞ for the Maxwell-type interface. The matrix is subjected to σ_{zx}^{∞} with the other fixed parameters $\chi = 1$ and $\mu_1 = 5\mu_2$. At the initial time $t = 0$, the result is the same as that for a linear-spring-type interface (see Fig. 2 for $t = \infty$). With increasing time, the stress level within the inhomogeneity decreases. When $t \to \infty$, the stress within the inhomogeneity approaches zero, due to the fact that as $t \to \infty$, the interface will become traction-free and cannot transfer load from the matrix to the inhomogeneity.

Also, by using the Mori–Tanaka mean-field method, the time-dependent effective shear modulus of a composite containing

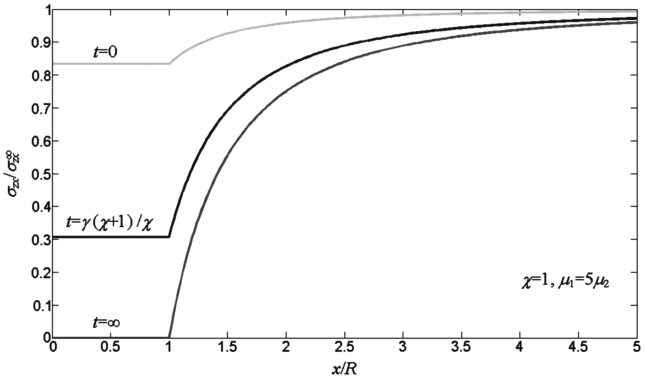

Fig. 4 Variation of σ_{zx} along the positive real axis at three different moments $[t = 0, [\gamma(\chi+1)]/\chi$, and $\infty]$ for the Maxwell-type interface, in which the matrix is subjected to σ_{zx}^{∞} with $\chi = 1$ and $\mu_1 = 5\mu_2$.

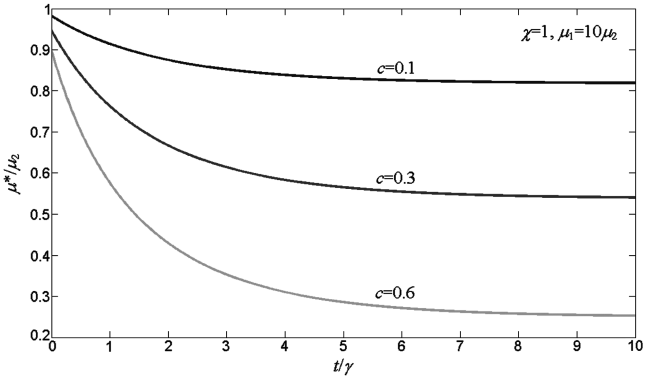

Fig. 5 Variation of μ^* as a function of time t for the Maxwell-type viscoelastic interface with $\chi = 1$ and $\mu_1 = 10\mu_2$.

randomly aligned fibers of the same radius with the Maxwell-type interface on the x–y plane can be derived as

$$\mu^* = \mu_2 \frac{1 - c\left[1 - \frac{2\chi\mu_1}{(\chi+1)(\mu_1+\mu_2)}\exp\left(-\frac{\chi t}{\gamma(\chi+1)}\right)\right]}{1 + c\left[1 - \frac{2\chi\mu_1}{(\chi+1)(\mu_1+\mu_2)}\exp\left(-\frac{\chi t}{\gamma(\chi+1)}\right)\right]} \tag{34}$$

Apparently, when $\chi \to \infty$, Eq. (34) is reduced to that derived by He and Kim [3]. Figure 5 illustrates the variation of μ^* as a function of time t for the Maxwell-type interface with $\chi = 1$ and $\mu_1 = 10\mu_2$. As expected μ^* changes from the result for a linear spring at $t = 0$ to that for a completely debonded interface at $t = \infty$.

V. Conclusions

We study an isolated circular inhomogeneity with a viscoelastic interface under remote uniform antiplane shear stresses. Exact closed-form solutions for both the Kelvin-and Maxwell-type viscoelastic interfaces are derived by means of the complex variable method. It is found that the complex variable method is very efficient in treating this quasi-static problem. The time-dependent stress and displacement fields in the inhomogeneity and the matrix are given. The derived solutions are also used to predict the effective shear modulus of the fiber-reinforced composite, which is important in the study of the time-dependent response of composites. The method presented here could be extended to address the interface described by a standard linear solid model, which combines the Maxwell model and a linear spring in parallel. In this study, we restrict our attention to the simple case in which both the inhomogeneity and matrix are assumed to be linearly elastic. A viscoelastic inhomogeneity and/or matrix [15,16] still remains a challenge.

It is well known that the mismatch of material properties at the fiber-matrix interface causes performance deterioration in composites. For example, it causes stress rise at the interface, phonon scattering in thermal transport, etc. The gradient morphology concept potentially provides a materials solution to address this particular issue (e.g., [17]). The gradient materials property distribution at the composite interface could be achieved through nanotechnology (carbon nanotubes, nanofibers, nanolayers, and buckypapers). This would require a functionally gradient interface to also incorporate the time-dependent behavior, which forms yet another challenge problem for the further endeavor.

Acknowledgments

This work was supported in part by U.S. Air Force Research Laboratory grant 06-S531-060-C1.

References

[1] Donaldson, S. L., and Roy, A. K., "Experimental Studies on Composite Bonded Joints," *Textile Composites and Characterization (ICCM-11)*, Vol. 5, Australian Composite Structures Society, Victoria, Australia, and Woodhead, Cambridge, England, U.K., July 1997, pp. 444–455.

[2] He, L. H., "Transient Stress Relaxation Around a Spherical Inclusion by Interfacial Diffusion and Sliding," *Acta Mechanica*, Vol. 149, Nos. 1–4, 2001, pp. 115–133. doi:10.1007/BF01261667

[3] He, L. H., and Lim, C. W., "Time-Dependent Interfacial Sliding in Fiber Composites Under Longitudinal Shear," *Composites Science and Technology*, Vol. 61, No. 4, 2001, pp. 579–584. doi:10.1016/S0266-3538(00)00237-2

[4] Suo, Z. G., "Motion of Microscopic Surface in Materials," *Advances in Applied Mechanics*, Vol. 33, 1997, pp. 193–294.

[5] Hashin, Z., "Composite Materials with Viscoelastic Interphase: Creep and Relaxation," *Mechanics of Materials*, Vol. 11, No. 2, 1991, pp. 135–148. doi:10.1016/0167-6636(91)90013-P

[6] Fan, H., and Wang, G. F., "Interaction Between a Screw Dislocation and Viscoelastic Interfaces," *International Journal of Solids and Structures*, Vol. 40, No. 4, 2003, pp. 763–776. doi:10.1016/S0020-7683(02)00553-X

[7] Ang, W. T., and Fan, H., "A Hypersingular Boundary Integral Method for Quasistatic Antiplane Deformations of an Elastic Bimaterial with an Imperfect and Viscoelastic Interface," *Engineering Computations*, Vol. 21, Nos. 5–6, 2004, pp. 529–539. doi:10.1108/02644400410543940

[8] Im, S. H., and Huang, R., "Evolution of Wrinkles in Elastic-Viscoelastic Bilayer Thin Films," *Journal of Applied Mechanics*, Vol. 72, 2005, pp. 955–961. doi:10.1115/1.2043191

[9] Yan, W., Chen, W. Q., and Wang, B. S., "On Time-Dependent Behavior of Cross-Ply Laminated Strips with Viscoelastic Interfaces," *Applied Mathematical Modelling*, Vol. 31, No. 2, 2007, pp. 381–391. doi:10.1016/j.apm.2005.11.014

[10] Ang, W. T., "Elastodynamic Antiplane Deformation of a Bimaterial with an Imperfect Viscoelastic Interface: a Dual Reciprocity Hypersingular Boundary Integral Equation," *Applied Mathematical Modelling*, Vol. 31, No. 4, 2007, pp. 749–762. doi:10.1016/j.apm.2005.12.007

[11] Mori, T., and Tanaka, K., "Average Stress in Matrix and Average Energy of Materials with Misfitting Inclusions," *Acta Metallurgica*, Vol. 21, No. 5, 1973, pp. 571–574. doi:10.1016/0001-6160(73)90064-3

[12] Weng, G. J., "Some Elastic Properties of Reinforced Solids, with Special Reference to Isotropic Ones Containing Spherical Inclusions," *International Journal of Engineering Science*, Vol. 22, No. 7, 1984, pp. 845–856. doi:10.1016/0020-7225(84)90033-8

[13] Ru, C. Q., and Schiavone, P., "A Circular Inclusion with Circumferentially Inhomogeneous Interface in Antiplane Shear," *Proceedings of the Royal Society of London A*, Vol. 453, No. 1967, 1997, pp. 2551–2572.

[14] Muskhelishvili, N. I., *Some Basic Problems of the Mathematical Theory of Elasticity*, P. Noordhoff, Ltd., Netherlands, 1963.

[15] Allam, M. N. M., and Appleby, P. G., "On the Plane Deformation of Fiber-Reinforced Viscoelastic Plate," *Applied Mathematical Modelling*, Vol. 9, No. 5, 1985, pp. 341–346. doi:10.1016/0307-904X(85)90021-6

[16] Allam, M. N. M., Zenkour, A. M., and El-Meckawy, H. F., "Stress Concentration in a Viscoelastic Composite Plate Weakened by a Triangular Hole," *Composite Structures*, Vol. 79, No. 1, 2007, pp. 1–11. doi:10.1016/j.compstruct.2005.11.023

[17] Pan, E., and Roy, A. K., "A Simple Plane-Strain Solution for Functionally Graded Multilayered Isotropic Cylinder," *Structural Engineering and Mechanics*, Vol. 24, No. 6, 2006, pp. 727–740.

K. Shivakumar
Associate Editor